A Structural Study of Tris(β-diketonate)europium(III) Complexes in Solution Using Magnetic Circularly Polarized Luminescence Spectroscopy

Frederick S. Richardson* and Harry G. Brittain

Contribution from the Department of Chemistry, University of Virginia, Charlottesville, Virginia 22901. *Received February 25, 1980*

Abstract: Total luminescence (TL) and magnetic circularly polarized luminescence (MCPL) spectra are reported for four tris(β-diketonate)europium(III) chelates dissolved in dimethyl sulfoxide (Me_2SO) and dimethylformamide (DMF) solvents. These spectra were recorded over the $^5D_0 \rightarrow {}^7F_J$ ($J = 0$–4) Eu(III) emission regions with applied magnetic field strengths varying from 0 to 4.2 T. The total luminescence spectra showed no magnetic field dependence, and the MCPL spectra can be interpreted entirely in terms of Faraday *B* terms associated with nondegenerate crystal field transitions. From these results it is deduced that each of the four Eu(β-diketonate)$_3$ chelate systems has a nonaxially symmetric structure in Me_2SO and DMF solvents. Further analysis of the $^5D_0 \rightarrow {}^7F_1$ MCPL/TL spectra leads to estimates of the magnitudes of the nonaxial crystal field interaction components.

I. Introduction

The spectroscopic and magnetic properties of β-diketonate complexes with trivalent lanthanide ions (Ln^{3+}) have been studied extensively. Motivation for many of the spectroscopic studies has been provided by the potential of these systems as lasing materials and as photosensitizing agents.[1-5] Interest in the magnetic properties has, in large part, been stimulated by the discovery that these systems can be used as paramagnetic shift reagents in nuclear magnetic resonance spectroscopy.[6] In this latter application, the Ln(β-diketonate) complex is presumed to coordinate weakly to a nucleophilic group of one or more substrate molecules, thus subjecting the magnetic nuclei of the substrate molecule(s) to strong perturbations originating with the paramagnetic ground state of the lanthanide ion. The stereospecific chemical shifts induced in the NMR spectra of the substrate molecules by these perturbations have proved to be of enormous value in sorting out and interpreting the NMR spectra of complex organic molecules and in obtaining detailed stereochemical and conformational structure information.[7-10] There are, however, a number of problems associated with constructing reliable spectra–structure relationships suitable for interpreting the NMR spectra obtained on lanthanide shift reagent (LSR)/substrate systems. One concerns the basic mechanism responsible for the magnetic perturbation. That is, what is the detailed nature of the Ln^{3+}–substrate molecule interaction? Another problem concerns the stoichiometry of the LSR/substrate complexes in solution as a function of [LSR]:[substrate] concentration ratios and as a function of solvent type. Yet another problem arises regarding the structural (stereochemical) properties of the LSR and of the LSR/substrate adducts in solution. Questions regarding the magnetic perturbation mechanisms and LSR/substrate stoichiometries have received considerable attention elsewhere and are not directly relevant to the study reported here. In the present study, we address one aspect of the last problem cited above. More specifically, we present data relevant to ascertaining the structural properties of the tris(β-diketonate)Ln(III) class of lanthanide shift reagents in solution.

Common to most of the analyses carried out on the NMR spectra of LSR/substrate systems is the assumption of axial symmetry in the LSR/substrate adduct structures. This assumption greatly simplifies the geometrical factor appearing in the dipolar shift expression for the paramagnetically perturbed NMR spectra and leads to particularly simple spectra–structure relationships. The correctness of this assumption has been called into question by Horrocks and co-workers,[11-13] who have cited solid-state structural and magnetic (anisotropy) susceptibility data to show that, in fact, most LSR's of the Ln(β-diketonate)$_3$ class do *not* possess axial symmetry—at least, not in the solid state. These workers have discussed the complications that arise when structural and/or magnetic axiality *cannot* be assumed and have suggested means for dealing with systems having nonaxial symmetry (i.e., no C_n symmetry axis, where $n > 2$).

In our laboratory, we have carried out a number of emission studies on the tris(β-diketonate) complexes of Eu^{3+} and Tb^{3+} to probe the structural properties of these complexes and their adducts in solution media.[14-17] These studies have included circularly polarized luminescence (CPL) measurements on chiral chelates in achiral solvents[14] and on achiral chelates in chiral solvents.[15] They have also included investigations of Tb(chelate) → Eu(chelate) energy transfer processes using luminescence intensity and lifetime measurement techniques.[16] These emission studies have yielded information regarding chelate–chelate interactions, chelate–solvent adduct formation, and lanthanide optical activity mechanisms. Emission spectroscopy provides a facile technique for probing the solution structures of the europium(III) and terbium(III) β-diketonate chelates. With near-ultraviolet excitation, the luminescence quantum yields of these systems are relatively high in a wide variety of nonaqueous solvents, and favorable emission detection sensitivity thresholds permit studies to be conducted at concentrations well below where chelate–chelate association (dimer or oligomer formation) becomes significant.

Emission studies of the Eu(III) chelates are especially productive because the emitting state in solution media at room temperature

(1) Crosby, G. A.; Kasha, M. *Spectrochim. Acta* **1958**, *10*, 377.
(2) Crosby, G. A.; Whan, R. E.; Alire, R. M. *J. Chem. Phys.* **1961**, *34*, 743.
(3) Crosby, G. A.; Whan, R. E.; Freeman, J. J. *J. Phys. Chem.* **1962**, *66*, 2493.
(4) Whan, R. E.; Crosby, G. A. *J. Mol. Spectrosc.* **1962**, *8*, 315.
(5) Sinha, A. P. B. In "Spectroscopy in Inorganic Chemistry"; Rao, C. N. R., Ferraro, J. R., Eds.; Academic Press: New York, 1971, Vol. II pp 255–288.
(6) Hinckley, C. C. *J. Am. Chem. Soc.* **1969**, *91*, 5160.
(7) Stevens, R. E., Ed. "Nuclear Magnetic Resonance Shift Reagents"; Academic Press: New York, 1973.
(8) Kime, K. K.; Sievers, R. E. *Aldrichimica Acta* **1977**, *10*, 54.
(9) Cockerill, A. F.; Davies, G. L. O.; Harden, R. C.; Rackham, D. M. *Chem. Rev.* **1973**, *73*, 553.
(10) Reuben, J. *Prog. Nucl. Magn. Reson. Spectrosc.* **1975**, *9*, 1.
(11) Horrocks, W. D., Jr.; Sipe, J. P. *Science (Washington, D.C.)* **1972**, *177*, 994.
(12) Horrocks, W. D., Jr. *J. Am. Chem. Soc.* **1974**, *96*, 3022.
(13) Horrocks, W. D. Jr.; Sipe, J. P.; Sudnick, D. In "Nuclear Magnetic Resonance Shift Reagents"; Sievers, R. E.; Ed.; Academic Press: New York 1973, pp 53–86.
(14) Brittain, H. G.; Richardson, F. S. *J. Am. Chem. Soc.* **1976**, *98*, 5858.
(15) Brittain, H. G.; Richardson, F. S. *J. Am. Chem. Soc.* **1977**, *99*, 65.
(16) Brittain, H. G.; Richardson, F. S. *J. Chem. Soc., Faraday Trans. 2* **1977**, *73*, 545.
(17) Brittain, H. G.; Richardson, F. S. *J. Chem. Soc., Dalton Trans.* **1976**, 2253.

0002-7863/81/1503-18$01.00/0

Table I. Symmetry Species Associated with Splittings of the ^7F_J Term Levels of Eu(III) in Trigonal Crystal Fields

crystal field sym	term levels (^7F_J)				
	$^7F_0$	$^7F_1$	$^7F_2$	$^7F_3$	$^7F_4$
D_{3h}	A'_1	A'_2, E"	A'_1, E', E"	A'_2, $A"_1$, $A"_2$, E', E"	A'_1, $A"_1$, $A"_2$, 2E', E"
D_3	A_1	A_2, E	A_1, 2E	A_1, $2A_2$, 2E	$2A_1$, A_2, 3E
C_{3h}	A'	A', E"	A', E', E"	A', 2A", E', E"	A', 2A", 2E', E"
C_{3v}	A_1	A_2, E	A_1, 2E	A_1, $2A_2$, 2E	$2A_1$, A_2, 3E
C_3	A	A, E	A, 2E	3A, 2E	3A, 3E

is $^5D_0$ which is nondegenerate and, therefore, remains unsplit in crystal fields of all symmetry types. The initial state in all of the visible region emissions of Eu(III), $^5D_0 \rightarrow {}^7F_J$ (J = 0, 1, 2, 3, or 4), retains its simple single-level structure no matter what the crystal field symmetry might be. Any splitting observed in the $^5D_0 \rightarrow {}^7F_0$ emission band can be taken as evidence either for strong Eu(III)–Eu(III) interactions due to chelate–chelate association or for heterogeneity with respect to the chelate structural species present in solution. The $^5D_0 \rightarrow {}^7F_1$ emission band of Eu(III) in monomeric chelates can be split, at most, into three crystal field components, and if axial symmetry exists, it will split into just two crystal field components. The $^5D_0 \rightarrow {}^7F_2$ emission of monomeric Eu(III) chelates will exhibit five crystal field components in nonaxial symmetry and, at most, three crystal field components if axial symmetry obtains. The $^5D_0 \rightarrow {}^7F_J$ emission spectra of Eu(III) chelates remain, then, relatively simple even in the presence of low-symmetry crystal fields. If the crystal field components of the Eu(III) $^5D_0 \rightarrow {}^7F_J$ emission bands can be resolved, it should be possible to determine the axial or nonaxial symmetry of the chelate structures. Furthermore, such an analysis should also reveal the presence of dimeric or oligomeric chelate species.

Even though the crystal field splittings of the $^5D_0 \rightarrow {}^7F_J$ Eu(III) emissions are predicted to be relatively simple, in solution spectra they are generally too small to allow complete resolution of the component crystal field emission bands (for $J \neq 0$). In many solvents, the Eu(β-diketonate)$_3$ chelate emission spectra show partial resolution, but the resolution is not sufficiently good to allow unambiguous counting or assigning of crystal field components. In the present study, we have turned to magnetic circularly polarized luminescence (MCPL) as a technique to help achieve a crystal field resolution of the emission spectra. MCPL is just the emission analogue of magnetic circular dichroism (MCD), and its theory and applications have been discussed previously.[18,19] In the MCPL experiment, a static magnetic field is applied to the sample with the magnetic field direction aligned parallel to the direction of emission collection and detection. The application of the magnetic field in this configuration will cause the sample to emit light which is elliptically polarized (that is, unequal amounts of left and right circularly polarized light). The emitted light is analyzed in terms of a circular intensity differential, $\Delta I = I_L - I_R$, and in terms of total intensity, $I = I_L + I_R$, where $I_{L(R)}$ is the intensity of the left (right) circularly polarized component of the emitted light. Since ΔI is a signed quantity whereas I is not, it may be expected that two closely spaced, strongly overlapping emission bands which remain unresolved in the total emission spectrum (I vs. λ) may be clearly resolved in the MCPL spectrum (ΔI vs. λ), if they have oppositely signed ΔI values.

In MCPL (and MCD) spectroscopy, the principal influences of the applied magnetic field are to (1) split degenerate states into their Zeeman sublevels and (2) mix the zero-field eigenstates of the system. Zeeman splitting of degenerate ground and excited states gives rise, respectively, to the so-called Faraday C and A terms in the standard perturbation theory of MCPL (and MCD).[18] Field-induced mixing of the field-free eigenstates of a system is reflected in the Faraday B term. In the present study we shall not attempt a detailed analysis of the MCPL spectra in terms of a full characterization of the spectroscopic states involved. Instead, we shall be interested in using MCPL to obtain crystal field resolutions of the observed emission bands and to ascertain the axiality or nonaxiality of the Eu(β-diketonate) chelate structures present in solution. The MCPL theory relevant to these objectives is given in the next section (vide infra).

Chart I

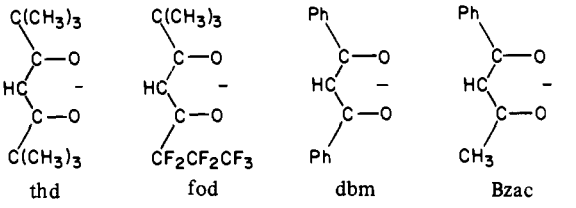

Four different tris(β-diketonate)europium(III) chelates are examined in this study. The β-diketonate ligands in these chelates are 2,2,6,6-tetramethyl-3,5-heptanedionate (thd), 6,6,7,7,8,8,8-heptafluoro-2,2-dimethyl-3,5-octanedionate (fod), dibenzoylmethanate (dbm), and 1-benzoylacetonate (Bzac). The structures of these ligands are shown in Chart I, where Ph denotes a phenyl substituent. These ligands differ with respect to symmetry and substituents. The tris(thd) and tris(fod) complexes of Eu(III) and Pr(III) are among the most commonly used LSR's in nonaqueous solutions.

Total emission studies of Eu(thd)$_3$, Eu(fod)$_3$, Eu(dbm)$_3$, and Eu(Bzac)$_3$ were carried out in dimethyl sulfoxide (Me_2SO) and dimethylformamide (DMF) solutions with chelate concentrations of 2 mM. Previous studies have shown that at these concentration levels in Me_2SO and DMF there is negligible chelate–chelate association.[16,17] Furthermore, there is some evidence that the Eu(thd)$_3$ and Eu(fod)$_3$ systems form 1:2 (and possibly some 1:3) chelate–solvent adduct species in Me_2SO and DMF. This adduct formation is promoted by the strong nucleophilicity of the solvent >C=O (DMF) and >S=O (Me_2SO) groups. The total emission spectra of the chelates in Me_2SO were found to be qualitatively identical with (and quantitatively very similar to) the spectra obtained in DMF. MCPL/emission spectra are reported, therefore, only for the chelate/DMF systems.

II. Symmetry Restrictions on MCPL/Emission Spectra

The highest symmetry permissible in the Eu(thd)$_3$ and Eu(dbm)$_3$ chelates is D_{3h}, while the highest symmetry permissible in the Eu(fod)$_3$ and Eu(Bzac)$_3$ chelates is C_{3v}. The symmetry species of the levels split out of the Eu(III) ^7F_J (J = 0–4) terms in five different trigonally symmetric crystal fields are given in Table I. The crystal field symmetry of the $^5D_0$ emitting state is, of course, in each case identical with that of the $^7F_0$ state. In Table II are listed the symmetry species of the ^7F_J (J = 0–4) crystal field levels of Eu(III) which are connected to the $^5D_0$ state via either electric dipole (ed) or magnetic dipole (md) moment operators. The numbers of allowed electric dipole and magnetic dipole crystal field transitions are given in Table III.

Application of a magnetic field to the Eu(β-diketonate)$_3$ systems will cause a splitting of each of the degenerate levels or transitions listed in Tables I and II. The magnitude of this (Zeeman) splitting will be, at low field strengths, linearly proportional to the magnetic field strength and the intrinsic magnetic moment of the degenerate state. The applied magnetic field will also induce mixings between the zero-field eigenstates of the system and will cause shifts in the energy eigenvalues of these states. The extent to which the magnetic field effects will be apparent in the total luminescence spectra of the Eu(III) $^5D_0 \rightarrow {}^7F_J$ transitions will depend upon (1)

(18) Riehl, J. P.; Richardson, F. S. *J. Chem. Phys.* **1977**, *66*, 1988.
(19) Richardson, F. S.; Riehl, J. P. *Chem. Rev.* **1977**, *77*, 773.

Table II. Allowed Electric Dipole (ed) and Magnetic Dipole (md) $^5D_0 \rightarrow {}^7F_J$ Transitions of Eu(III) in Trigonal Crystal Fields

term levels	crystal field sym				
	D_{3h}	D_3	C_{3h}	C_{3v}	C_3
$^7F_0$			A'(md)	A_1(ed)	A(ed)
$^7F_1$	A'$_2$(md)	A_2(ed,md)	A'(md)	A_2(md)	A(ed,md)
	E"(md)	E(ed,md)	E"(md)	E(ed,md)	E(ed,md)
$^7F_2$	E'(ed)	2E(ed,md)	A'(md)	A_1(ed)	A(ed,md)
	E"(md)		E'(ed)	2E(ed,md)	2E(ed,md)
			E"(md)		
$^7F_3$	A'$_2$(md)	$2A_2$(ed,md)	A'(md)	A_1(ed)	3A(ed,md)
	A"$_2$(ed)	2E(ed,md)	2A"(ed)	$2A_2$(md)	2E(ed,md)
	E'(ed)		E'(ed)	2E(ed,md)	
	E"(md)		E"(md)		
$^7F_4$	A"$_2$(ed)	A_2(ed,md)	A'(md)	$2A_1$(ed)	3A(ed,md)
	2E'(ed)	3E(ed,md)	2A"(ed)	A_2(md)	3E(ed,md)
	E"(md)		2E'(ed)	3E(ed,md)	
			E"(md)		

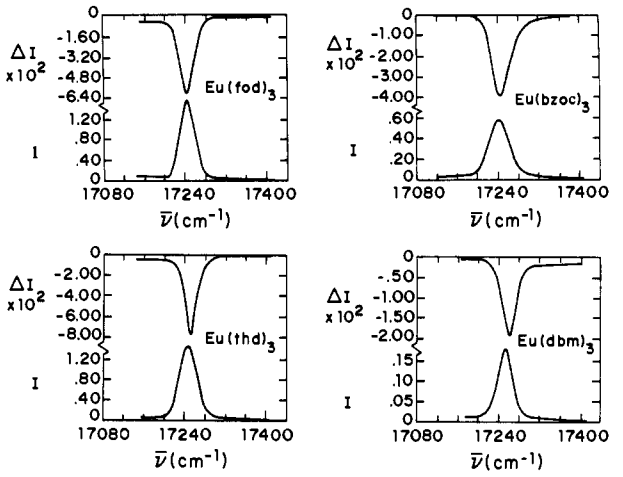

Figure 1. MCPL (ΔI) and total luminescence (I) spectra in the $^5D_0 \rightarrow {}^7F_0$ transition region of Eu(β-diketonate)$_3$ complexes dissolved in pure DMF solvent (magnetic field strength = 4.2 T). The ΔI and I intensity scales are expressed in the (arbitrary) units used in Figure 3.

the symmetry of the zero-field crystal field Hamiltonian, $\mathcal{H}_{cf}$, (2) the magnitude of the applied field strength, H, and (3) the *relative* magnitudes of $\mathcal{H}_{cf}$ and $g\mu_B H$, where μ_B is the Bohr magneton and g is the gyromagnetic factor for the optical electron. If $\mathcal{H}_{cf}$ has nonaxial symmetry (no zero-field degeneracies) and if $\mathcal{H}_{cf} \gg g\mu_B H$, then the magnetic field effects on the total luminescence spectra are expected to be very weak. If, on the other hand, $\mathcal{H}_{cf}$ has trigonal symmetry and $\mathcal{H}_{cf} \approx g\mu_B H$, then Zeeman splittings within the degenerate transitions should be readily observable and perturbations on the intensities and energies of all other transitions may be observed. What can be observed in cases falling between these two extremes is difficult to predict.

The qualitative and quantitative aspects of the Eu(III) $^5D_0 \rightarrow {}^7F_J$ MCPL spectra will also depend upon the symmetry of $\mathcal{H}_{cf}$ and the relative magnitudes of $\mathcal{H}_{cf}$ vs. $g\mu_B H$. For the case where $\mathcal{H}_{cf}$ is axially symmetric and $\mathcal{H}_{cf} > g\mu_B H$, the MCPL spectra can be readily analyzed in terms of the traditional Faraday A, B, and C parameters. If $\mathcal{H}_{cf}$ is nonaxially symmetric and $\mathcal{H}_{cf} \gg g\mu_B H$, the MCPL spectra can be analyzed entirely in terms of Faraday B parameters, one associated with each nondegenerate crystal field transition.

In the present study, we qualitatively analyze the MCPL/total luminescence (TL) spectra according to the following characteristics (or cases).

Case I. No magnetic field effects are apparent in the TL spectra and the MCPL spectra are describable entirely in terms of Faraday B parameters. This would correspond to $\mathcal{H}_{cf} > g\mu_B H$, with $\mathcal{H}_{cf}$ having nonaxial symmetry. In this case, the intensities but *not* the energies of the MCPL bands should exhibit a field dependence.

Case II. Magnetic field induced splittings are observed in the TL spectra, and Faraday A terms are observed in the MCPL spectra. Both the TL and MCPL spectra exhibit strong field dependence. This case corresponds to an axially symmetric $\mathcal{H}_{cf}$.

Case III. Both the TL and MCPL spectra exhibit field dependence (in band energies and/or intensities), but no Faraday A terms are observed. This case would correspond to a nonaxially symmetric $\mathcal{H}_{cf}$ but would also indicate that $\mathcal{H}_{cf}$ (nonaxially symmetric components) is small compared to $g\mu_B H$.

Classification of the Eu(β-diketonate)$_3$ complexes according to whether their MCPL/TL spectra conform to cases I, II, or III should provide unambiguous evidence regarding their axial or nonaxial symmetry. Furthermore, the splittings and field dependencies observed in their MCPL/TL spectra can be used to estimate the magnitudes of possible nonaxial crystal field components. A detailed analysis of how the MCPL/TL spectra conforming to cases I, II, and III may be interpreted within the $^5D_0 \rightarrow {}^7F_1$ transition region is given in the Appendix of this paper.

III. Experimental Section

The four chelates Eu(thd)$_3$, Eu(fod)$_3$, Eu(dbm)$_3$, and Eu(Bzac)$_3$ (see Introduction for the full names of these chelates) were purchased from Aldrich Chemical Co. Studies were carried out with these chelates dissolved in either dimethyl sulfoxide (Me_2SO) or dimethylformamide (DMF). The Me_2SO and DMF solvents were of spectroquality, and great care was taken to ensure that they were anhydrous. Chelate concentrations were 2 mM in all the studies reported here.

The MCPL/TL experiments were carried out with the samples contained in an insulated cell placed in the bore of a superconducting magnet (Oxford Instruments). Sample temperature was maintained at ~298 K in all of the experiments. Sample luminescence was excited with the 350.7-nm line of a continuous-wave krypton ion laser, and the MCPL and TL spectra were recorded simultaneously by using an emission spectrophotometer constructed in this laboratory.[19] Magnetic field strengths from 0 to 4.2 T were employed. Sample luminescence was measured over the 17 100–14 000-cm^{-1} spectral range, corresponding to Eu(III) $^5D_0 \rightarrow {}^7F_0$, $^7F_1$, $^7F_2$, $^7F_3$, and $^7F_4$ emission. The power output of the laser was 50 mW at the 350.7-nm exciting line, and no photodecomposition of the samples was observed to take place under the experimental conditions employed in this study.

IV. Results

The MCPL and TL spectra obtained at 4.2 T are displayed in Figures 1–5. All of the spectra shown in these figures were

Table III. Number of Allowed Electric Dipole (ed) and Magnetic Dipole (md) Crystal Field Components in the Eu(III) $^5D_0 \rightarrow {}^7F_J$ Transitions[a]

crystal field sym	term levels (^7F_J)				
	$^7F_0$	$^7F_1$	$^7F_2$	$^7F_3$	$^7F_4$
D_{3h}	0	2md	1ed + 1md	2ed + 2md	3ed + 1md
D_3	0	2b	2b	4b	4b
C_{3h}	1md	2md	1ed + 2md	3ed + 2md	4ed + 2md
C_{3v}	1ed	1b + 1md	2b + 1ed	2b + 1ed + 2md	3b + 3ed + 1md
C_3	1ed	2b	3b	5b	6b
nonaxial[b]	1	3	5	7	9

[a] ed denotes electric dopole allowedness, md denotes magnetic dipole allowedness, and b denotes *both* electric dipole and magnetic dipole allowedness. [b] In this case, the electric dipole allowedness and magnetic dipole allowedness of a given transition will depend upon which nonaxial crystal field point group is being considered. We list the *total* number of a crystal field components allowed in crystal fields having at most *one* C_2 rotation axis

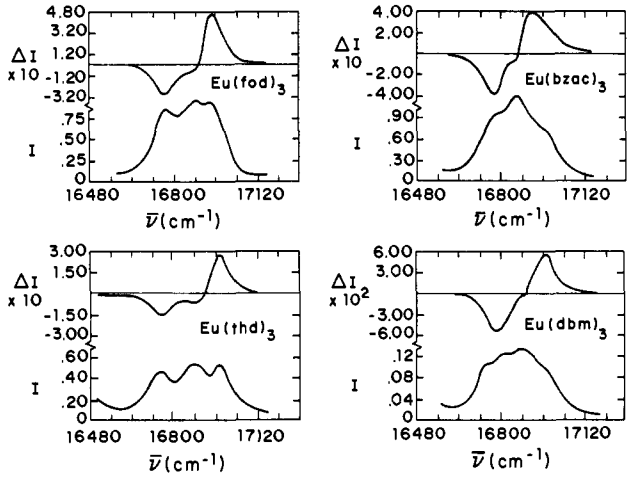

Figure 2. MCPL (ΔI) and total luminescence (I) spectra in the $^5D_0 \rightarrow {}^7F_1$ transition region of Eu(β-diketonate)$_3$ complexes dissolved in pure DMF solvent (magnetic field strength = 4.2 T). The ΔI and I intensity scales are expressed in the (arbitrary) units used in Figure 3.

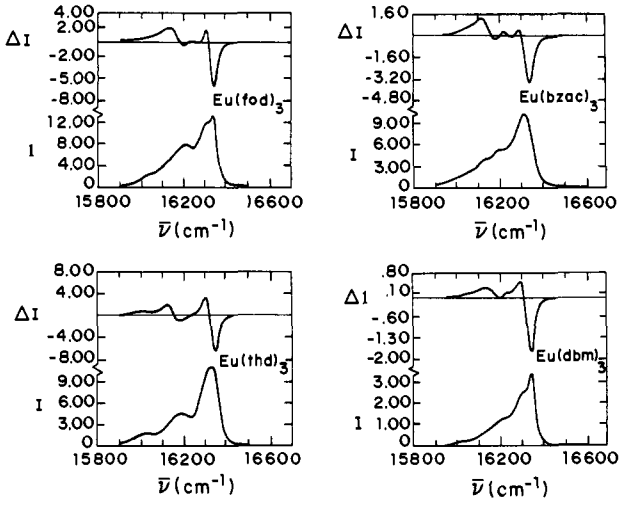

Figure 3. MCPL (ΔI) and total luminescence (I) spectra in the $^5D_0 \rightarrow {}^7F_2$ transition region of Eu(β-diketonate)$_3$ complexes dissolved in pure DMF solvent (magnetic field strength = 4.2 T). The ΔI and I intensity scales are expressed in arbitrary units.

obtained on samples with 2 mM chelate concentration in pure DMF solvent. Except for small differences in intensity, the analogous spectra obtained for chelate/Me_2SO systems were identical (i.e., the number of bands and the band splitting patterns observed in Me_2SO vs. DMF solvent were identical).

In varying the applied magnetic field stength from 0 to 4.2 T, we observed *no changes* in the TL spectra of any of the four chelate systems studied. The intensities (ΔI) of the bands appearing in the MCPL spectra were found to have approximately linear dependence on the applied field strength, but no field-induced splittings or field-induced band shifts were observed in the MCPL spectra. The MCPL/TL spectra for each of the four chelate systems clearly conform to *case I* conditions described in section II of this paper (vide supra).

V. Discussion

The first, and major, conclusion to be drawn from the results presented in section IV (Results) is that in DMF (and Me_2SO) *none* of the four tris(β-diketonate)europium(III) chelates have axial symmetry. Furthermore, these results suggest that the nonaxial components of the crystal field about the Eu(III) chromophore are sufficiently strong to "quench" all magnetic field effects *except* that responsible for the Faraday B term contributions to the MCPL spectra. The MCPL spectra can be analyzed entirely on the basis of Faraday B terms associated with nondegenerate crystal field transitions. The absence of any splitting

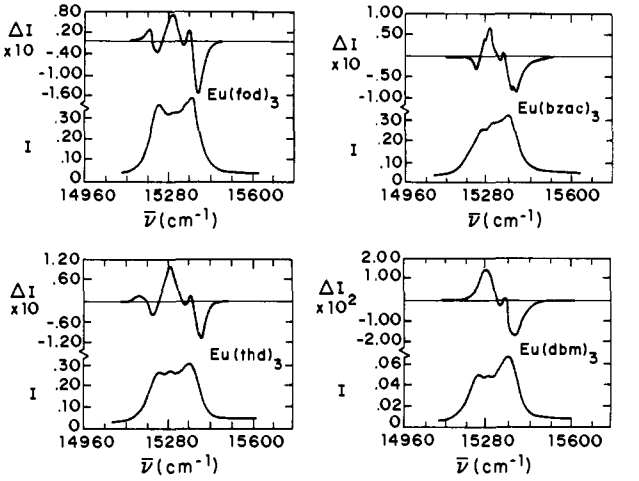

Figure 4. MCPL (ΔI) and total luminescence (I) spectra in the $^5D_0 \rightarrow {}^7F_3$ transition region of Eu(β-diketonate)$_3$ complexes dissolved in pure DMF solvent (magnetic field strength = 4.2 T). The ΔI and I intensity scales are expressed in the (arbitrary) units used in Figure 3.

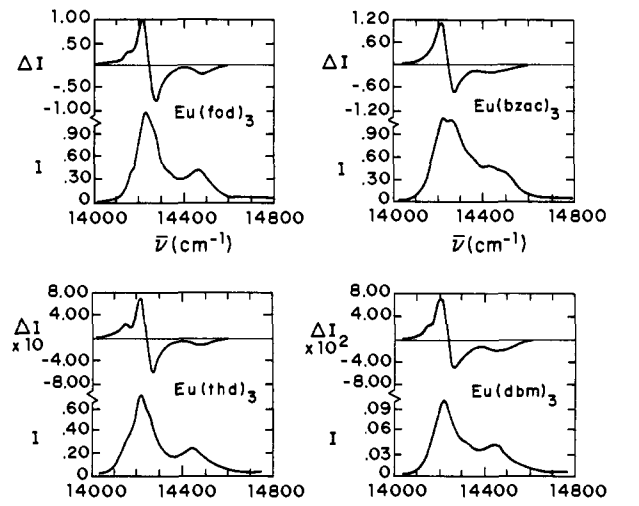

Figure 5. MCPL (ΔI) and total luminescence (I) spectra in the $^5D_0 \rightarrow {}^7F_4$ transition region of Eu(β-diketonate)$_3$ complexes dissolved in pure DMF solvent (magnetic field strength = 4.2 T). The ΔI and I intensity scales are expressed in the (arbitrary) units used in Figure 3.

in the observed $^5D_0 \rightarrow {}^7F_0$ emissions further indicates that only single structural species exist in solution and that these species are monomeric chelates.

Case I behavior of the MCPL/TL spectra obtained for each of the four Eu(III) chelate systems clearly demonstrates that the nonaxially symmetric components of the crystal fields created by the ligands are dominant over the axially symmetric components. It is of further interest, however, to estimate the approximate strengths of the nonaxially symmetric crystal field components. This can be done in a rough way by applying the analysis given in the Appendix to the $^5D_0 \rightarrow {}^7F_1$ MCPL/TL spectra shown in Figure 2.

For case I behavior without any $H_{cf}(2,1)$ crystal field components, the $^5D_0 \rightarrow {}^7F_1$ TL spectrum is predicted to consist of three bands of approximately equal intensity and with uniform energy spacings equal to $|\Delta_1(2,2)|$. The corresponding MCPL spectrum is predicted to exhibit two bands of opposite sign and equal intensity centered at $\pm\Delta_1(2,2)$ from the center band of the TL spectrum. The spacing between the two MCPL band maxima is predicted to be $2|\Delta_1(2,2)|$. The MCPL/TL spectra of Figure 2 conform rather closely to the predictions for "ideal" case I behavior, although there are some deviations which vary from chelate to chelate. These deviations include nonuniform energy spacings and intensity distributions among the three TL bands

Table IV. Observed Energy Splittings between the $|x\rangle$ and $|y\rangle$ Orthorhombic Crystal Field Components of the $^7F_1$ Term Level and Calculated Values of $|B_2^{(2)}|$

chelate	energy splitting[a]/cm^{-1}	$\lvert B_2^{(2)}\rvert$[b]/cm^{-1}
Eu(thd)$_3$	235	655
Eu(fod)$_3$	190	530
Eu(dbm)$_3$	205	572
Eu(Bzac)$_3$	165	460

[a] Estimated from the MCPL/TL spectra of Figure 2. [c] Calculated from eq 2 with $|2\Delta_1(2,2)|$ = observed energy splitting.

and the appearance of weak MCPL in the center band. Each of the observed deviations from "ideal" case I behavior can be accounted for in terms of small (but nonnegligible) effects due to $H_{cf}(2,0)$, $H_{cf}(2,1)$, or crystal field induced J–J' mixing. It is likely that all three of these effects are operative to some extent but their deconvolution would require an analysis beyond the scope of the present study. Evidence for nonnegligible J–J' mixing is provided by the observation of MCPL intensity in the $^5D_0 \rightarrow {}^7F_0$ transition. If the chelate structure has at least one C_2 symmetry axis, then the nonaxial crystal field component $H_{cf}(2,1)$ is rigorously zero.

Assuming nearly "ideal" case I behavior, we can estimate the value of the energy parameter $\Delta_1(2,2)$ by measuring the energy separation between the two intense MCPL bands appearing with opposite signs in the spectra of Figure 2. This energy separation is approximately equal to $2|\Delta_1(2,2)|$. The energy parameter $\Delta_1(2,2)$ can be further related to the orthorhombic crystal field coefficient, $B_2^{(2)}$ of eq A2 in the Appendix, by eq 1, where

$$\begin{aligned}\Delta_1(2,2) &= B_2^{(2)}\langle x|(U_2^{(2)} + U_{-2}^{(2)})|x\rangle \\ &= -B_2^{(2)}(^7F_1\|U^{(2)}\|^7F_1)/5^{1/2}\end{aligned} \quad (1)$$

$(^7F_1\|U^{(2)}\|^7F_1)$ is the reduced matrix element of the operator $U^{(2)}$ within the $^7F_1$ term level. Considering only LS coupling and taking $^7F_1$ to be a pure Russell–Saunders state, we may readily evaluate the reduced matrix element in eq 1 to yield a value of $3/56^{1/2}$. Using this value and rearranging eq 1 gives eq 2. Observed values of $2|\Delta_1(2,2)|$ and calculated values for $|B_2^{(2)}|$ are listed in Table IV.

$$B_2^{(2)} = -\frac{2(70)^{1/2}}{3}\Delta_1(2,2) \simeq -5.5777\Delta_1(2,2) \quad (2)$$

From the observed values of $2|\Delta_1(2,2)|$, we can also estimate the magnitude of the perturbation coefficient, ϵ, defined by eq A8 of the Appendix. Taking a value of 1.5 for g, appropriate for pure LS coupling, we have eq 3, where H is expressed in tesla and $\Delta_1(2,2)$ in cm^{-1}. For H = 4.2 T (the maximum field strength used in our studies) and $|2\Delta_1(2,2)|$ = 200 cm^{-1}, the value of $|\epsilon|$ is 1.47×10^{-2}.

$$|\epsilon| = 0.7003H/|2\Delta_1(2,2)| \quad (3)$$

The sign of $\Delta_1(2,2)$ and, therefore, of $B_2^{(2)}$ cannot be determined from our MCPL/TL spectra in the $^5D_0 \rightarrow {}^7F_1$ emission region. This sign information can only be obtained from a more complete analysis of the overall spectra. Detailed analyses of the $^5D_0 \rightarrow {}^7F_J$ ($J \neq 1$) MCPL/TL spectra have not been carried out in the present study. However, it is clear that they follow case I behavior and their splitting patterns require the dominance of nonaxially symmetric crystal field components over axially symmetric components.

VI. Conclusions

The major conclusion to be drawn from this work is that the Eu(thd)$_3$, Eu(fod)$_3$, Eu(dbm)$_3$, and Eu(Bzac)$_3$ chelates each have nonaxially symmetric structures in pure Me_2SO and DMF solvents. The MCPL/TL spectra obtained for these chelates afforded complete resolution of the crystal field components associated with the $^5D_0 \rightarrow {}^7F_J$ (J = 0–3) emissive transition of Eu(III). A more detailed (but still approximate) analysis of the $^5D_0 \rightarrow {}^7F_1$ MCPL spectra led to an estimate of the strength of the leading nonaxial crystal field interaction term operative within the various chelate systems.

Acknowledgment. This work was supported by grants from the National Science Foundation (Grant CHE77-02150) and the Camille and Henry Dreyfus Foundation (through a Teacher-Scholar Award to F.S.R.).

Appendix. Magnetic Field and Low-Order Crystal Field Effects on the $^5D_0 \rightarrow {}^7F_1$ Transition of Eu(III)

To illustrate the effects of crystal fields and externally applied magnetic fields on the $^5D_0 \rightarrow {}^7F_J$ emissive transitions of Eu(III), we present here an analysis of the $^5D_0 \rightarrow {}^7F_1$ transition by using approximations appropriate to the systems and experimental conditions employed in this study. Analyses for the $^5D_0 \rightarrow {}^7F_J$ ($J \neq 0$ or 1) transitions would follow similar procedures, but the details would be somewhat more complicated.

Free-Ion Wave Functions and Energy Levels. In the absence of crystal fields and externally applied magnetic fields, the 4f electron wave functions of the Eu(III) "free ion" may be represented in intermediate-coupling notation as $|\psi[SL]JM_J\rangle$, where ψ denotes a collection of quantum numbers and seniority labels not dependent upon J and M_J and where the brackets enclosing SL indicate that neither S nor L is a "good" quantum number (owing to strong spin–orbit coupling). Only J and M_J remain "good" angular momentum quantum numbers and state energies depend only upon ψ and J, with each free-ion energy level being $(2J + 1)$-fold degenerate. In the present discussion, we shall denote the energy of the $^5D_0$ emitting state of Eu(III) as E°_0 and the free-ion wave function of this state as $|\psi'0,0\rangle$. The energy of the $^7F_1$ level will be denoted by E°_1 and the wave functions by $|\psi 1,M_J\rangle$ where $M_J = 0, \pm 1$.

Crystal Field and Magnetic Field Effects on Free-Ion Energy Levels and Wave Functions. In considering crystal field and magnetic field perturbations on the free-ion wave functions and energy levels, we shall retain J as a "good" quantum number (thus ignoring all J–J' mixing) and we shall neglect the spherically symmetric component of the crystal field potential. Under these conditions, the $^5D_0$ state remains entirely unaffected by either a crystal field or an externally applied magnetic field.

The Hamiltonian operator for the externally applied magnetic field (i.e., the Zeeman operator) may be written as eq A1, where

$$\mathcal{H}_{ze} = \mu_B \mathbf{H}\cdot(\mathbf{L} + 2\mathbf{S}) \quad (A1)$$

μ_B is the Bohr magneton and H is the applied magnetic field vector. Choosing an axis of quantization parallel to the direction of the applied magnetic field, the operator $\mathcal{H}_{ze}$ is diagonal in M_J with eigenvalues $M_J g\mu_B H$, where g is the gyromagnetic factor for a 4f electron and H is the magnitude of H. The influence of $\mathcal{H}_{ze}$ upon the $^7F_1$ free-ion state is to split it into its three Zeeman sublevels according to

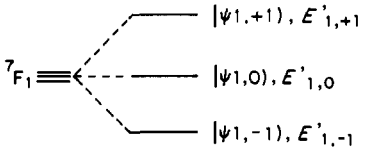

where $E'_{1,0} = E^\circ_1$ and $E'_{1,\pm 1} = E^\circ_1 \pm g\mu_B H$.

The lowest order even-parity terms appearing in the crystal field Hamiltonian (excluding the spherically symmetric term) are displayed as eq A2, where the $B_q^{(k)}$ are crystal field expansion

$$\begin{aligned}\mathcal{H}_{cf} &= B_0^{(2)}U_0^{(2)} + B_1^{(2)}(U_{-1}^{(2)} - U_1^{(2)}) + B_2^{(2)}(U_2^{(2)}) + U_{-2}^{(2)} \\ &= H_{cf}(2,0) + H_{cf}(2,1) + H_{cf}(2,2)\end{aligned} \quad (A2)$$

coefficients and the $U_q^{(k)}$ are the standard intraconfigurational unit tensor operators.[20] The first term in eq A2 is axially symmetric and is diagonal in M_J. The second and third terms are nonaxially symmetric and neither is diagonal in M_J. The second term mixes M_J levels according to $|\Delta M_J| = 1$, and the third term

(20) Wybourne, B. G. "Spectroscopic Properties of Rare Earths"; Wiley-Interscience: New York, 1965.

mixes M_J levels according to $|\Delta M_J| = 2$. In considering the influence of $\mathcal{H}_{cf}$ on the $^7F_1$ free-ion level, it will be convenient to redefine the basis states of $^7F_1$ as $|\psi 1,z) = |\psi 1,0) = |z\rangle$, $|\psi 1,x) = N[|\psi 1,+1) - |\psi 1,-1)] = |x\rangle$, and $|\psi 1,y) = iN[|\psi 1,+1) + |\psi 1,-1)] = |y\rangle$, where N is a normalization factor defined to be real. (We shall set $N = 2^{-1/2}$ in the following development.) The operator $H_{cf}(2,2)$ is diagonal in this new basis set with eigenvalues $E_z(2,2) = 0$ and $E_x(2,2) = -E_y(2,2) = \Delta_1(2,2)$, where $\Delta_1(2,2) = \langle x|H_{cf}(2,2)|x\rangle$. The off-diagonal matrix elements of $H_{cf}(2,0)$ in this basis set are pure imaginary and have no influence on the $^7F_1$ energy levels. The diagonal elements of $H_{cf}(2,0)$ in the new basis set are given by $E_z(2,0) = \Delta_1(2,0)$ and $E_x(2,0) = E_y(2,0) = -{}^1/_2\Delta_1(2,0)$, where $\Delta_1(2,0) = \langle z|H_{cf}(2,0)|z\rangle$.

The $H_{cf}(2,1)$ operator is entirely off diagonal in the $|x\rangle$, $|y\rangle$, and $|z\rangle$ basis. Its effect is to mix $|z\rangle$ with both $|x\rangle$ and $|y\rangle$ but not $|x\rangle$ with $|y\rangle$. We shall proceed by assuming that $H_{cf}(2,1)$ is much smaller than either $H_{cf}(2,2)$ or $H_{cf}(2,0)$ and treat its influence on the $^7F_1$ energy levels by second-order perturbation theory. Denoting the second-order energy corrections to the $|x\rangle$, $|y\rangle$, and $|z\rangle$ eigenstates of $H_{cf}(2,0) + H_{cf}(2,2)$ by $E''_x(2,1)$, $E''_y(2,1)$, and $E''_y(2,1)$, respectively, we have

$$E''_x = \frac{\langle x|H_{cf}(2,1)|z\rangle\langle z|H_{cf}(2,1)|x\rangle}{\Delta_1(2,2) - (3/2)\Delta_1(2,0)}$$

$$E''_y = \frac{\langle y|H_{cf}(2,1)|z\rangle\langle z|H_{cf}(2,1)|y\rangle}{-\Delta_1(2,2) - (3/2)\Delta_1(2,0)}$$

$$E''_z = -E''_x - E''_y$$

With these energy corrections to the crystal field sublevels of $^7F_1$, we may write the wave functions and associated energies as eq A3–A5, where primes on x, y, and z indicate some admixture of $|z\rangle$ into $|x\rangle$ and $|y\rangle$ (and vice versa) via $H_{cf}(2,1)$.

$$|z'\rangle,\ E_{z'} = E^\circ{}_1 + \Delta_1(2,0) - E''_x - E''_y \quad \text{(A3)}$$

$$|x'\rangle,\ E_{x'} = E^\circ{}_1 - {}^1/_2\Delta_1(2,0) + \Delta_1(2,2) + E''_x \quad \text{(A4)}$$

$$|y'\rangle,\ E_{y'} = E^\circ{}_1 - {}^1/_2\Delta_1(2,0) - \Delta_1(2,2) + E''_y \quad \text{(A5)}$$

With respect to the influence of the crystal field, two special cases are of particular interest here. In one case, $H_{cf}(2,0) \gg H_{cf}(2,2) \approx H_{cf}(2,1)$. In this case, $E''_x \approx E''_y$ and $E''_z \approx -2E''_x$, and the crystal field is dominated by the axially symmetric component. In the other case, $H_{cf}(2,2) \gg H_{cf}(2,0) \approx H_{cf}(2,1)$. In this case, $E''_x \approx -E''_y$ and $E''_z \approx 0$, and the crystal field is dominated by the nonaxially symmetric orthorhombic component $H_{cf}(2,2)$. The qualitative splitting patterns expected within the $^7F_1$ state for these two special cases are depicted below.

For the case $H_{cf}(2,0) >> H_{cf}(2,2) \approx H_{cf}(2,1)$:

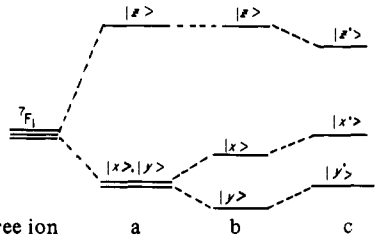

where (a) $H_{cf}(2,2) = H_{cf}(2,1) = 0$, (b) $H_{cf}(2,1) = 0$, and (c) all components are *nonzero*.

For the case $H_{cf}(2,2) >> H_{cf}(2,0) \approx H_{cf}(2,1)$:

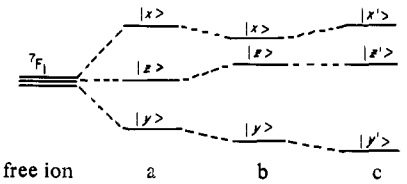

where (a) $H_{cf}(2,0) = H_{cf}(2,1) = 0$, (b) $H_{cf}(2,1) = 0$, and (c) all components are *nonzero*.

As noted previously, the Zeeman Hamiltonian is diagonal in M_J with eigenvalues $M_J g\mu_B H$. In the (x, y, z) basis, it leaves $|z\rangle$ unchanged but it mixes $|x\rangle$ and $|y\rangle$ to produce the (first-order) perturbed states

$$|x''\rangle = |x\rangle - i\epsilon|y\rangle \quad \text{(A6)}$$

$$|y''\rangle = |y\rangle - i\epsilon|x\rangle \quad \text{(A7)}$$

where ϵ is a real quantity whose magnitude depends upon the applied field strength (H) and the energy separation between the field-free $|x\rangle$ and $|y\rangle$ states. More explicity, the perturbation parameter ϵ is given by eq A8. Ignoring $H_{cf}(2,1)$, we have $(E_x - E_y) \approx 2\Delta_1(2,2)$. To second order in ϵ, the energies of the $|z''\rangle$, $|x''\rangle$, and $|y''\rangle$ states are given by eq A9–A12. When $|\Delta_1(2,2)| \gg g\mu_B H$, we have $\epsilon^2 \ll 1$, and eq A12 becomes eq A13. Under these conditions the orthorhombic crystal field, $H_{cf}(2,2)$, and the applied magnetic field, $\mathcal{H}_{ze}$, make *additive* contributions to $E_{x''} - E_{y''}$, with $H_{cf}(2,2)$ being dominant. For $\epsilon^2 \gg 1$, eq A12 becomes eq A14 and in this case $H_{cf}(2,2)$ and $\mathcal{H}_{ze}$ make oppositely signed contributions to $E_{x''} - E_{y''}$.

$$\epsilon = g\mu_B H/(E_x - E_y) \quad \text{(A8)}$$

$$E_{z''} = E^\circ{}_1 + \Delta_1(2,0) \quad \text{(A9)}$$

$$E_{x''} = E^\circ{}_1 - {}^1/_2(1 + \epsilon^2)\Delta_1(2,0) + (1 - \epsilon^2)\Delta_1(2,2) + 2\epsilon g\mu_B H \quad \text{(A10)}$$

$$E_{y''} = E^\circ{}_1 - {}^1/_2(1 + \epsilon^2)\Delta_1(2,0) - (1 - \epsilon^2)\Delta_1(2,2) - 2\epsilon g\mu_B H \quad \text{(A11)}$$

$$E_{x''} - E_{y''} = 2(1 - \epsilon^2)\Delta_1(2,2) + 4\epsilon g\mu_B H \quad \text{(A12)}$$

$$E_{x''} - E_{y''} \simeq 2\Delta_1(2,2) + 4\epsilon g\mu_B H = 2\Delta_1(2,2) + \frac{2(g\mu_B H)^2}{\Delta_1(2,2)} \quad \text{(A13)}$$

$$E_{x''} - E_{y''} \simeq -2\epsilon^2\Delta_1(2,2) + 4\epsilon g\mu_B H \quad \text{(A14)}$$

In the (x', y', z') basis with $H_{cf}(2,1) \neq 0$, the $\mathcal{H}_{ze}$ operator will mix all three states and will perturb the z' energy level as well as the x' and y' energy levels.

$^5D_0 \rightarrow {}^7F_1$ Magnetic Dipole Transitions. In the free-ion approximation, the $^5D_0 \rightarrow {}^7F_1$ transition of Eu(III) is magnetic dipole allowed but electric dipole forbidden (by parity). Even in noncentrosymmetric crystal fields this transition retains its strong (and dominant) magnetic dipole character, and we shall consider only the magnetic dipole transition mechanism here. We denote the spherical components of the magnetic dipole transition vector by $\hat{m}_0$, $\hat{m}_+$, and $\hat{m}_-$ and consider transitions between the $^5D_0$ emitting state and the $|z''\rangle$, $|x''\rangle$, and $|y''\rangle$ sublevels of the $^7F_1$ state. Ignoring $H_{cf}(2,1)$, we take $|x''\rangle$ and $|y''\rangle$ as defined by eq A6 and A7 and define $|z''\rangle = |z\rangle$. Writing the $^5D_0$ state function as $|0\rangle$, we obtain the expressions for the *nonvanishing* components of $\langle {}^5D_0|\hat{m}|{}^7F_1\rangle$

$$\langle 0|\hat{m}_+|x''\rangle = (\epsilon - 1)\langle 0|\hat{m}_+|-1\rangle/2^{1/2}$$

$$\langle 0|\hat{m}_-|x''\rangle = (\epsilon + 1)\langle 0|\hat{m}_-|+1\rangle/2^{1/2}$$

$$\langle 0|\hat{m}_+|y''\rangle = i(\epsilon + 1)\langle 0|\hat{m}_+|-1\rangle/2^{1/2}$$

$$\langle 0|\hat{m}_-|y''\rangle = -i(\epsilon - 1)\langle 0|\hat{m}_-|+1\rangle/2^{1/2}$$

$$\langle 0|\hat{m}_0|z''\rangle = \langle 0|\hat{m}_0|0\rangle$$

where the numbers in kets $(0,\pm 1)$ refer to M_J values within $^7F_1$. The analogous component (magnetic) dipole strength quantities are given as follows: $D_+(0,x') = (\epsilon^2 - 2\epsilon + 1)M^2/2$, $D_-(0,x') = (\epsilon^2 + 2\epsilon + 1)M^2/2$; $D_+(0,y'') = (\epsilon^2 + 2\epsilon + 1)M^2/2$, $D_-(0,y'') = (\epsilon^2 - 2\epsilon + 1)M^2/2$; $D_0(0,z'') = M^2$ (where $M^2 = |\langle 0|\hat{m}_0|0\rangle|^2$). From these expressions, the total magnetic dipole strengths may be written as eq A15 and A16. These dipole strengths will govern

$$D(0,x'') = D(0,y'') = (\epsilon^2 + 1)M^2 \quad \text{(A15)}$$

$$D(0,z'') = M^2 \quad \text{(A16)}$$

the total (unpolarized) emission intensities of the $0 \rightarrow j$ (x'', y'', and z'') transitions according to eq A17, where $\bar{\nu}_{0j}$ is the transition frequency.

$$I \propto \bar{\nu}_{0j}{}^4 D(0,j) \tag{A17}$$

The magnetic circularly polarized luminescence (MCPL) intensity (ΔI) of the $0 \rightarrow j$ transition will be governed by eq A18.[18]

$$\Delta I \propto \bar{\nu}_{0j}{}^4 [D_-(0,j) - D_+(0,j)] \tag{A18}$$

We have, then, for the $|0\rangle \rightarrow |x''\rangle$, $|y''\rangle$, and $|z''\rangle$ $^5D_0 \rightarrow {}^7F_1$ transitions

$$\Delta I(0,x'') \propto 2\bar{\nu}_{0x''}{}^4 \epsilon M^2 \tag{A19}$$

$$\Delta I(0,y'') \propto -2\bar{\nu}_{0y''}{}^4 \epsilon M^2 \tag{A20}$$

$$\Delta I(0,z'') = 0 \tag{A21}$$

The influence of $H_{cf}(2,1) \neq 0$ on the intensity analysis A6–A8), above would be to (1) redistribute the total luminescence intensity (I) among the $|0\rangle \rightarrow |x''\rangle$, $|y''\rangle$, and $|z''\rangle$ transitions causing some intensity asymmetry between the $|0\rangle \rightarrow |x''\rangle$ and $|0\rangle \rightarrow |y''\rangle$ transitions and (2) induce some MCPL intensity (ΔI) in the $|0\rangle \rightarrow |z''\rangle$ transition as well as causing $|\Delta I(0,x'')| \neq |\Delta I(0,y'')|$.

Given our first-order treatment of magnetic field effects (see eq A6–A8), eq A19 and A20 show MCPL intensity to be linear in the magnetic field strength H. On the other hand, eq A15–A17 show that the total luminescence intensities will exhibit a field dependence only when $|\epsilon| \rightarrow 1$ (i.e., when $|\Delta_1(2,2)| \approx g\mu_B H$).

Classification of Spectra According to Cases I, II, and III of Section II (See Main Text). In section II of the main text three special cases are defined for the purpose of classifying the observed MCPL/TL spectra obtained for the Eu(β-diketonate)$_3$ systems. This is a relatively "low-resolution" classification scheme with respect to making spectra–structure correlations, but it suffices for distinguishing between dominant axial or dominant nonaxial symmetry in the systems under study. Here we apply this classification scheme to the $^5D_0 \rightarrow {}^7F_1$ transition by using the analysis developed in this Appendix. Neglecting the low-symmetry $H_{cf}(2,1)$ crystal field component, we can make the following comments regarding cases I, II, and III.

Case I. This case corresponds to $H_{cf}(2,2) \gg H_{cf}(2,0)$ and $|\epsilon| \ll 1$. The TL spectrum should show three well-resolved bands with energies and relative intensities given by

$\|0\rangle \rightarrow \|j\rangle$	$\|\Delta E_{0j}\|$	$I(0,j)/\bar{\nu}_{0j}{}^4$
$\|0\rangle \rightarrow \|x''\rangle$	$\|E_1^\circ + \Delta_1(2,2)\|$	M^2
$\|0\rangle \rightarrow \|y''\rangle$	$\|E_1^\circ - \Delta_1(2,2)\|$	M^2
$\|0\rangle \rightarrow \|z''\rangle$	$\|E_1^\circ\|$	M^2

The MCPL spectrum should show just to well-resolved bands with intensities $\Delta I(0,x'') \propto 2\bar{\nu}_{0x''}{}^4 \epsilon M^2$ and $\Delta I(0,y'') \propto -2\bar{\nu}_{0y''}{}^4 \epsilon M^2$. This case also admits $H_{cf}(2,1) \neq 0$, the effects of which are to give the $|0\rangle \rightarrow |z''\rangle$ transition some (weak) MCPL intensity and to cause both intensity and transition energy asymmetry in the TL spectrum.

Case II. This case corresponds to $H_{cf}(2,0) \gg H_{cf}(2,2)$ and $|\epsilon| > 1$. In this case both the TL and MCPL spectra should exhibit a strong magnetic field dependence according to

$\|0\rangle \rightarrow \|j\rangle$	$\|\Delta E_{0j}\|$	$I(0,j)/\bar{\nu}_{0j}{}^4$	$\Delta I(0,j)/\bar{\nu}_{0j}{}^4$
$\|0\rangle \rightarrow \|x''\rangle$	$\|E_1^\circ - {}^1/_2(1+\epsilon^2)\Delta_1(2,0) + 2g\mu_B H\epsilon\|$	$(\epsilon^2+1)M^2$	$2\epsilon M^2$
$\|0\rangle \rightarrow \|y''\rangle$	$\|E_1^\circ - {}^1/_2(1+\epsilon^2)\Delta_1(2,0) - 2g\mu_B H\epsilon\|$	$(\epsilon^2+1)M^2$	$-2\epsilon M^2$
$\|0\rangle \rightarrow \|z''\rangle$	$\|E_1^\circ + \Delta_1(2,0)\|$	M^2	0

The energy separation between the $|0\rangle \rightarrow |x''\rangle$ and $|0\rangle \rightarrow |y''\rangle$ transitions is linearly dependent upon $H\epsilon$, collapsing to (near) zero when $H = 0$. In this case, corresponding to the presence of a very strong axially symmetric crystal field component, both the transition frequencies and the intensity distributions within the $^5D_0 \rightarrow {}^7F_1$ TL spectrum will exhibit a strong magnetic field dependence.

Case III. This case corresponds to $H_{cf}(2,2) > H_{cf}(2,0)$ and $|\epsilon| > 1$. In this case the transitions are characterized approximately by

$\|0\rangle \rightarrow \|j\rangle$	$\|\Delta E_{0j}\|$	$I(0,j)/\bar{\nu}_{0j}{}^4$	$\Delta I(0,j)/\bar{\nu}_{0j}{}^4$
$\|0\rangle \rightarrow \|x''\rangle$	$\|E_1^\circ + (1-\epsilon^2)\Delta_1(2,2) + 2g\mu_B H\epsilon\|$	$(\epsilon^2+1)M^2$	$2\epsilon M^2$
$\|0\rangle \rightarrow \|y''\rangle$	$\|E_1^\circ - (1-\epsilon^2)\Delta_1(2,2) - 2g\mu_B H\epsilon\|$	$(\epsilon^2+1)M^2$	$-2\epsilon M^2$
$\|0\rangle \rightarrow \|z''\rangle$	$\|E_1^\circ\|$	M^2	0

From this analysis it is clear that the $|0\rangle \rightarrow |x''\rangle$ and $|0\rangle \rightarrow |y''\rangle$ components of the $^5D_0 \rightarrow {}^7F_1$ MCPL/TL spectra can provide effective probes of $H_{cf}(2,0)$ and $H_{cf}(2,2)$. The $|0\rangle \rightarrow |z''\rangle$ component can provide yet additional information about $H_{cf}(2,0)$ and $H_{cf}(2,2)$, as well as about $H_{cf}(2,1)$.

An Unexpectedly Strong Hydrogen Bond: Ab Initio Calculations and Spectroscopic Studies of Amide–Fluoride Systems

John Emsley,*[1a] Deborah J. Jones,[1a] Jack M. Miller,[1b] Richard E. Overill,[1c] and Roland A. Waddilove[1a]

Contribution from the Department of Chemistry and the Computer Unit of King's College, University of London, Strand, London WC2R 2LS, England, and the Department of Chemistry, Brock University, St. Catharines, Ontario, Canada L2S 3A1. *Received January 29, 1980*

Abstract: Ab inito LCAO–MO–SCF calculations have been performed on the formamide–fluoride, acetamide–fluoride and methylformamide–fluoride complexes to determine their equilibrium structures and the strength of the amide–fluoride hydrogen bond. At ca. 148 kJ mol^{-1} it is the second strongest hydrogen bond known. The results of IR, ^1H and ^{19}F NMR spectroscopic studies on solutions of alkali metal fluorides in these amides support this finding. Possible biochemical implications of this strong hydrogen bond are briefly discussed.

Strong hydrogen bonding is now recognized as a chemical interaction that is clearly distinguishable from normal hydrogen bonding by a variety of measurements: short bond lengths, high bond energies, large IR band shifts, and large downfield chemical

0002-7863/81/1503-24$01.00/0